Refractive Acoustic Devices for Airborne Sound

F. Cervera, L. Sanchis, J. V. Sánchez-Pérez, R. Martínez-Sala, C. Rubio, and F. Meseguer*
Centro Tecnológico de Ondas, Unidad Asociada de Investigación (CSIC-UPV), Edificio de Institutos II, Universidad Politécnica de Valencia, E-46022 Valencia, Spain

C. López
Instituto de Ciencia de Materiales de Madrid, Consejo Superior de Investigaciones Científicas, Cantoblanco, E-28049 Madrid, Spain

D. Caballero and J. Sánchez-Dehesa*
Departamento de Física Teórica de la Materia Condensada, Facultad de Ciencias (C-5), Universidad Autónoma de Madrid, E-28049 Madrid, Spain
(Received 8 May 2001; published 27 December 2001)

We show that a sonic crystal made of periodic distributions of rigid cylinders in air acts as a new material which allows the construction of refractive acoustic devices for airborne sound. It is demonstrated that, in the long-wave regime, the crystal has low impedance and the sound is transmitted at subsonic velocities. Here, the fabrication and characterization of a convergent lens are presented. Also, an example of a Fabry-Perot interferometer based on this crystal is analyzed. It is concluded that refractive devices based on sonic crystals behave in a manner similar to that of optical systems.

DOI: 10.1103/PhysRevLett.88.023902 PACS numbers: 43.20.+g, 43.58.+z, 43.90.+v

Optical refractive devices are possible for visible light because solid dielectric materials exist with the following two properties: (i) they transmit the light at a velocity c lower than that of air and (ii) they are transparent to electromagnetic (EM) waves in a certain frequency range. The last property is due to the fact that their EM impedance $Z = \mu c$ (μ is the magnetic permeability) is similar to that of air. As a consequence of the first property, a convergent lens has the familiar lenticular shape. In a similar manner, to construct acoustical devices for airborne sound one has to look for acoustical materials with the corresponding properties regarding sound propagation at audible wavelengths. Materials with a phase velocity larger than the sound speed in air ($v_{\text{air}} = 340$ m/s) could be used, but, the convergent lens would be concave. The acoustic impedance is defined as the product of the sound velocity v and mass density ρ; $Z = \rho v$. For solids (and liquids), Z is much larger than that of air because both v and ρ are larger also. Unfortunately, the transmittance at an air/solid interface is controlled by the ratio of their respective acoustic impedances $Z_{\text{air}}/Z_{\text{solid}}$. This fact impedes an efficient transmission of energy at the corresponding interfaces and makes the fabrication of acoustic refractive devices for airborne sound impracticable.

In this Letter we show that sonic crystals (SCs) [1] consisting of an array of rigid cylinders in air can be used to make such refractive devices. We present the physical realization of two devices commonly used in optics: a Fabry-Perot interferometer and a convergent lens.

The EM counterpart of SCs are called photonic crystals [2] and lattices of dielectric rods embedded in a background with a different dielectric constant have been proposed to build optical lenses [3]. No physical realization of such devices has been presented to date.

Arrays of sound scatterers with cylindrical shape in air have been widely studied previously [4–12]. Nevertheless, such work has been focused mainly on the study of spectral gaps for inhibition of sound transmission, looking for applications such as sound shields and acoustic filters. To the best of our knowledge this is the first work devoted to the study of SCs at wavelengths well below the first acoustic gap; i.e., in the frequency region where they are transparent to sound.

The fact that a periodic distribution of spherical solid scatterers in air constitutes a system in which the sound travels at subsonic velocity was proved by Meyer and Newmann; [13] basing their work on this fact, they constructed a prototype of converging lens by using disks as scatterers. However, the authors did not present experimental evidences of either the efficiency of such a device or any characterization of the physical parameters that control its performance. On the other hand, focusing effects can be obtained by using time-reversal techniques [14,15].

The SCs used in this work (see Fig. 1) consist of 1 m long cylindrical aluminum rods hanging from a frame with a hexagonal pattern that has a lattice constant $a = 6.35$ cm. The cylinder diameter d is varied in order to obtain structures with different filling fraction, whose value is $f = (\pi/2\sqrt{3})(d/a)^2$. Experiments have been performed with rods of $d = 1, 2, 3$, and 4 cm.

The measurements have been performed in an echo-free chamber. The sound velocity inside the samples is obtained by using the phase delay method in zero-order transmission experiments as described in Ref. [9]. Incident white sound is generated with frequencies in a

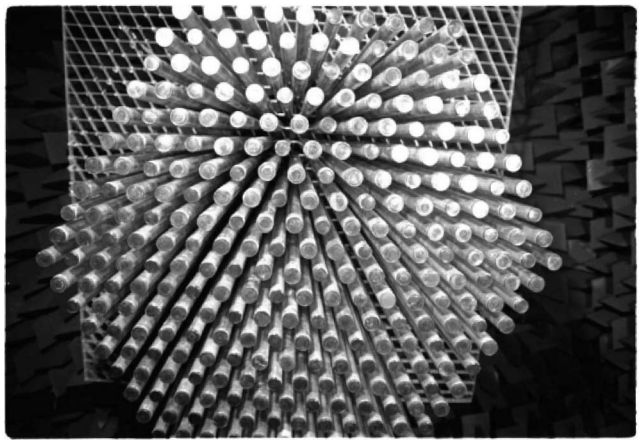

FIG. 1. Photograph of a typical sonic crystal sample taken from underneath. Part of the frame, the walls, and the ceiling of the echo-free chamber can also be seen.

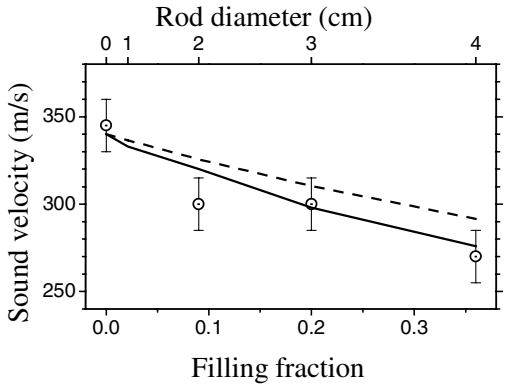

FIG. 2. Sound velocity as a function of the filling fraction or the rod diameter (top axis). Experimental values are represented by open circles whereas theoretical ones are shown by the solid line (full band structure calculation) or the dashed line [simple model of Eq. (2)].

wide region. A collimated beam is obtained by placing the speaker (5 cm of diameter size) at the focus of a parabolic reflector, which reflects the sound towards the structure. Microphones of 1 cm were used as receivers. The results were analyzed in a frequency region ($500 < \nu < 2000$ Hz) below the first band gap in all the structures, in other words, at frequencies where the phase velocity and group velocity coincide. The band gaps of these structures have been calculated and measured as in Ref. [7]. The structure having the smallest low frequency band edge was built with the largest diameter cylinders ($d = 4$ cm), and its gap spans the frequency range (2300–3300 Hz). The open circles in Fig. 2 represent the recorded velocities as a function of f (bottom axis) and rod diameter (top axis). Sound speeds are always lower than that in air and decrease when f increases.

Theoretically, two different methods were employed to compute the phase velocity in order to have physical insight of the origin of the observed behavior. First, we have calculated the full dispersion relation of the acoustic bands for the structures analyzed using the simplified approach of infinitely long cylinders and infinite periodic systems. This method involves the resolution of the following partial differential equation for sound propagation in a lossless fluid with mass density $\rho(\mathbf{r})$:

$$\vec{\nabla}[\rho^{-1}(\mathbf{r}) \cdot \vec{\nabla} p(\mathbf{r})] + \omega^2 \kappa(\mathbf{r}) p(\mathbf{r}) = 0, \qquad (1)$$

where $p(\mathbf{r})$ is the pressure, ω is the angular frequency, and $\kappa(\mathbf{r}) = [v^2(\mathbf{r})\rho(\mathbf{r})]^{-1}$ is the compressibility. This approach, which neglects mode conversion inside the solid cylinders, is valid in our case because of the high contrast in both velocities ($v_{al}/v_{\text{air}} \approx 20$) and mass densities ($\rho_{al}/\rho_{\text{air}} \approx 2100$). The corresponding huge impedance contrast between air and rod impedes the penetration of sound inside the solid and, then, the effect of transversal waves can be fully disregarded. In terms of scattering theory our approach is similar to studying sound propagation in a lossless fluid (air) with perfectly rigid and monodisperse scatterers (aluminum rods). A variational method is employed to solve the differential equation and details of the procedure can be found elsewhere [7]. The predicted sound velocities are obtained from the slope of the first acoustic band along the direction of detection. The values (solid line in Fig. 2) fairly match the experimental ones.

In spite of the fairly good agreement previously found, a simpler model can be used to explain the reduction of sound velocity within the SC. If an array of hard scatterers is rigidly fixed in an alternating pressure field, the incident wave and the scattered waves are superimposed in such a way that the sound propagation speed is reduced. In other words, the flowing medium effectively has an increased inertia or density. When dealing with rigid cylinders in an oscillating fluid (the sound field), we can make the problem equivalent to that of oscillating cylinders in air at rest [13]. The air around the oscillating cylinders impedes them from vibrating freely, and this impedance effect results in an effective increase of the density of the medium [13]. In this way, for a single cylinder, the mass per unit length increase equals the mass per unit length $S\rho_{\text{air}}$ of the air displaced by the cylinder [16], where $S = \pi R^2$ is the cross section of a cylinder and ρ_{air} is the air normal density. If N is the number of cylinders per unit area, then the increase in the effective density is given by $\rho_{\text{eff}} = \rho_{\text{air}} + N\rho_{\text{air}}S = \rho_{\text{air}}(1 + f)$. The phase velocity is inversely proportional to the square root of the density ρ_{eff} and the compressibility $\kappa_{\text{eff}} = \kappa_{\text{air}}$. Therefore, the sound speed in the SC, which is related to that in air through the refractive index, is

$$v_{\text{sc}} = v_{\text{air}}/n = v_{\text{air}}/\sqrt{1 + f}\,. \qquad (2)$$

In Fig. 2, the dashed line represents the velocity v_{sc} obtained with this simple model. Although the model is simple, the values agree qualitatively with those predicted by the band structure calculation.

From here on, we focus our discussion on the structure with the smallest sound velocity. It is made of cylinders having 4 cm of diameter and, according to the phase delay technique, the sound travels in this composite medium at a speed of 270 m/s. Its acoustic refractive index is 1.3 ± 0.1, a typical value in optical materials. However, this similarity does not guarantee that an acoustical material has a high transmittance, since this quantity is determined by the ratio of acoustic impedances. Therefore, an independent determination of its characteristic impedance Z_{sc} and a measurement of the reflectance is necessary.

In order to obtain those magnitudes we have fabricated a plane parallel sample which has a performance similar to a Fabry-Perot interferometer. It was made of 5 monolayers of cylinders (22 cm thickness) oriented along the ΓX direction in the hexagonal structure (see the inset in Fig. 3). The reflectance has been obtained by the standing wave ratio technique [17], which has been previously tested by us in studying these systems [12]. In short, this technique consists in the analysis of the oscillations in the reflectance R as a function of frequency when a sound flow impinges on the layer defined by the SC. The oscillations appear in the frequency region below 2300 Hz, the onset of the band gap (see the right panel in Fig. 3). In particular, the ones at low frequencies have an almost constant period and can be accounted for by the expression that gives the reflectance R by a homogenized layer of thickness L [17],

$$R = \frac{4R_o \sin^2(\omega L/v_{sc})}{1 + R_o^2 - 2R_o \cos(2\omega L/v_{sc})}, \qquad (3)$$

where $R_o = (Z_{sc} - Z_{air})^2/(Z_{sc} + Z_{air})^2$ is the reflectance at normal incidence at a single interface and v_{sc} is the phase velocity in the layer. The fit (solid line in Fig. 3) of the experimental data gives $c_{sc} = 230 \pm 40$ m/s and $R_o = 0.12 \pm 0.05$, from which a ratio $Z_{sc}/Z_{air} \approx 2.0$ is obtained. This procedure, which is an alternative to getting the phase velocity, confirms the value previously obtained by the phase velocity technique, which is the more accurate. Notice that the oscillation at frequencies close to the band gap (above 2000 Hz) has a shorter period and a large reflectance. This is a band structure effect; the slope of the acoustic band is no longer constant (see the left panel in Fig. 3) and the sound travels inside the structure at lower group velocity. On the other hand, the results at frequencies below 500 Hz (the cutoff frequency of the echo-free chamber) are not reliable.

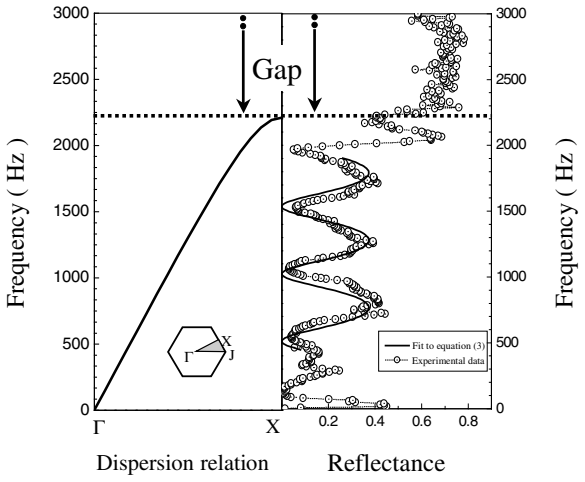

FIG. 3. Right panel: Reflectance spectrum (open circles) of a sonic crystal slab (5 monolayers) made of 4 cm diameter aluminum cylinders in a hexagonal configuration. The surfaces are oriented along the ΓX direction. Left panel: The corresponding acoustic band structure of the infinite structure calculated along the same direction (only the first band and part of the gap appear). The inset shows the first Brillouin zone, the shadowed region being its irreducible part.

In conclusion, the reflectance spectrum of the SC slab analyzed shows that it mimics the Fabry-Perot interferometer commonly used in optics. The small reflectance obtained, despite the high content of solid matter (36%), supports the suitability of our SC to make refractive devices in a manner entirely similar to that of optics.

To fabricate an acoustic convergent lens we followed the procedure employed for optical lenses in the microwave regime [18]. The lens profile is determined by calculating the acoustical path of rays that enter the lens parallel to the acoustical axis and converge, after traversing it, on a common point (focus) and equating it to a constant. To test such a lens we have used the computer positioning system previously developed by us [12], which allows the mapping of the sound level in a region 3.0×1.2 m^2 behind the sample. Figure 4 shows the design of a SC based biconvex lens and the corresponding pressure map (lower right) working at a frequency of 1700 Hz. For comparison purposes, we have also plotted (upper part) the design and pressure map of a SC slab with parallel surfaces. Both the slab and the lens sketches are drawn with the same scale as the pressure maps in order to facilitate their comparison. The origin of distances in the X direction has been taken

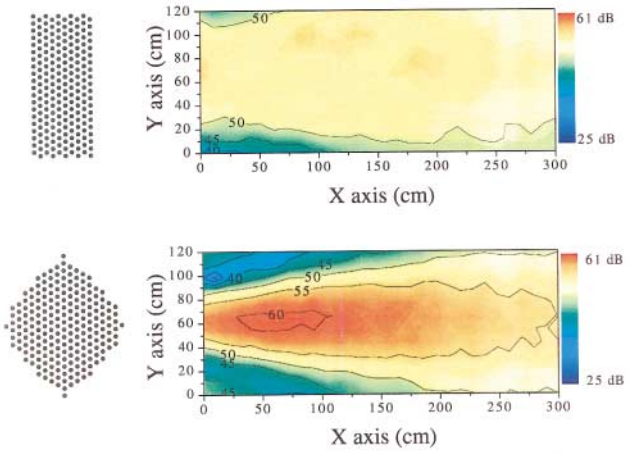

FIG. 4 (color). Sound level maps taken at 1700 Hz along with the samples' sketches. The sketches are drawn to scale: both samples are 1.2 m wide.

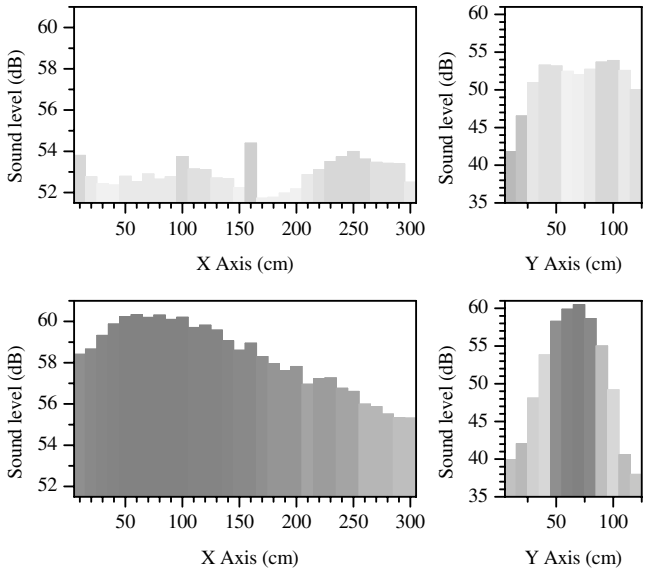

FIG. 5. Pressure profiles along (left) and across (right) the plane parallel slab (top) and lens (bottom), taken at 1700 Hz. The profiles are extracted from Fig. 4. The cross sections are taken at the focal distance.

at the lens apex in the symmetry axis of the system, which corresponds to the acoustical axis. One can see that, contrary to the plane parallel sample, which produces a rather uniform sound map, the pressure map from the lens shows a clear focusing effect. The concentration is more than 20 dB and can be felt by the naked ear. The focalization is then a direct consequence of the external shape of the sample. However, the finite lateral size of the lens (1.2 m) has two detrimental effects: it not only makes it effective in a limited wavelength range but some diffraction effects that can be seen in the map are attributable to edge effects. On the other hand, the short vertical dimension (the bars are 1 m long) can reduce the concentration performance due to the fact that the edges act as sound radiators [19].

The sound profiles along and across the acoustical axis are shown in Fig. 5 for the two systems analyzed in Fig. 4. The longitudinal sections clearly demonstrate that the lens configuration concentrates the sound with maximum effect (focal point) at a distance of about 70 cm. On the contrary, the plane parallel slab produces almost a uniform distribution of pressure, only slightly perturbed by diffraction. In the section taken across the acoustical axis this effect is even clearer. From the pressure pattern the effect of aberration can be appreciated. In our opinion, this can be attributed to the combined effects of two major factors: on the one hand, the numerical aperture is very large ($f/\# = 0.58$) which leads to broad foci and, on the other hand, the lens surface roughness is, by construction, comparable to the wavelength, which can also produce intense diffractive phenomena.

In summary, this work has demonstrated that sonic crystals made by two-dimensional arrays of rigid cylinders in air are new materials suitable for building up refractive devices in a manner similar to that of optics. A Fabry-Perot-like interferometer and a converging lens have been physically realized and tested. It has been shown that these materials have good energy transmission and that the speed of sound is lower than in air, which results in a behavior equivalent to EM waves propagating in a dielectric material: convex surfaces produce ray convergence. Further studies are needed to get an optimization of parameters for practical functioning devices.

Work partially supported by the Comisión Interministerial de Ciencia y Tecnología of Spain, Contract No. MAT2000-1670-C04. D. C. and J. S-D. acknowledge the computing facilities provided by the Centro de Computación Científica at the UAM.

*Author to whom correspondence should be addressed. Electronic mails: fmese@fis.upv.es; jose.sanchezdehesa@uam.es

[1] M. Sigalas and E. N. Economou, J. Sound Vib. **158**, 377 (1992); for a recent review, see M. S. Kushwaha, Recent Res. Devel. Appl. Phys. **2**, 743 (1999).
[2] J. D. Joannopoulous, R. D. Meade, and J. N. Winn, *Photonic Crystals* (Princeton University Press, Princeton, 1995).
[3] P. Halevi, A. A. Krokhin, and J. Arriaga, Phys. Rev. Lett. **82**, 719 (1999); Appl. Phys. Lett. **75**, 2725 (1999).
[4] R. Martínez-Sala *et al.,* Nature (London) **378**, 241 (1995).
[5] M. M. Sigalas and E. N. Economou, Europhys. Lett. **36**, 241 (1996).
[6] M. S. Kuswaha, Appl. Phys. Lett. **70**, 3218 (1997).
[7] J. V. Sánchez-Pérez *et al.,* Phys. Rev. Lett. **80**, 5325 (1998).
[8] W. M. Robertson and W. F. Rudy III, J. Acoust. Soc. Am. **104**, 694 (1998).
[9] C. Rubio *et al.,* J. Lightwave Technol. **17**, 2202 (1999).
[10] D. Caballero *et al.,* Phys. Rev. E **60**, R6316 (1999); Phys. Rev. B **64**, 064303 (2001).
[11] Y. Y. Chen and Z. Ye, Phys. Rev. Lett. **87**, 184301 (2001).
[12] L. Sanchis *et al.,* J. Acoust. Soc. Am. **109**, 2598 (2001).
[13] E. Meyer and E. G. Neumann, *Physical and Applied Acoustics* (Academic Press, New York, 1972).
[14] M. Fink *et al.,* Rep. Prog. Phys. **63**, 1933 (2000).
[15] A. Tourin, A. Derode, and M. Fink, Europhys. Lett. **47**, 175 (1999).
[16] P. M. Morse and K. U. Ingaard, *Theoretical Acoustic* (McGraw-Hill, New York, 1968).
[17] D. H. Towne, *Wave Phenomena* (Dover, New York, 1988).
[18] R. C. Johnson, *Antenna Engineering Handbook* (McGraw-Hill, New York, 1993).
[19] Z. Maekawa, Appl. Acoust. **1**, 157 (1968).